Defence Science Journal, Vol 45, No 2, April 1995, pp 107-116

Measurement of Microstructure of Snow from Surface Sections

M.Q. Edens and R.L. Brown

Civil Engineering Department, Montana State University, Bozeman, MT 59717, USA

ABSTRAC

A new approach to modelling the microstructure of snow is presented. The features involved in this formulation include skeletonising of the granular material and the modelling of the necks as a system of truncated cones. The skeletonising involves the process of representing the granular structure by a series of lines describing the grains and the necks and bonds. The value associated with any point on the skeleton is determined by the closest distance from the point to a grain boundary or neck boundary, whichever is smaller. This approach allows for easy visualisation of the material and for efficient data storage. The use of truncated cone model for the necked regions represents a more accurate physical description of the necks and should provide for a better relationship between microstructure and material properties. Preliminary results of one case study are presented.

1. INTRODUCTION

Many modern constitutive theories for granular materials consider the behaviour of the internal microstructure in their formulation. Brown[1], Hansen and Brown[2], Alley[3] and others have developed constitutive equations for snow which include consideration of the internal microstructure. Brown's constitutive theory[1] included the bond radius, neck length and coordination numbers as variables. These models depend upon the evolutionary behaviour of the microstructural variables included in the formulation. We are presently conducting research to develop evolution equations for several of these microstructural parameters. To support this work, an experimental program is being carried out to measure the microstructural changes occurring in snow undergoing large deformation. In a previous experimental study[4] data for snow subjected to large deformation and densification from 500 to 650 kg/m^3 were obtained. In that study, measurements of change in neck length yielded inconclusive results. This was due to insufficient image resolution and visual observation of each neck measured. That study pointed out the need for a method of feature detection which would apply definitions uniformly to every image, and which would reduce the time required to analyse a single surface section. This paper considers a method being implemented for automated detection and measurement of bonds and necks. The next section presents definitions of a bond, neck and neck length.

2 MECHANICAL BEHAVIOUR AND MICROSTRUCTURE

The behaviour of snow is dependent upon the organisation and properties of its internal structure. Its deformation characteristics depend upon the space available for grain movement, and the stresses transmitted from grain to grain. To characterise the largest stress states in the microstructure of snow, it is necessary to measure the bond radius. The largest stress concentrations will occur at the bond since its cross-sectional area is smaller than that of the associated grains. Due to the increased stress concentration throughout the neck region, any plastic flow which

Received 23 January 1995

occurs will generally occur here. Because of the high stresses in the bonds and the plastic flow in the neck regions, these regions will play a major role in determining the behaviour during loading. The changes in neck lengths are a measure of the plastic flow that has occurred while the changes in bond radius provide data on new bond formation, bond growth and breakage.

Another significant factor controlling the behaviour of snow is the number of bonds per grain (three-dimensional coordination number). As the number of bonds per grain increases, more load can be supported, thereby providing a mechanism for reducing the stress concentrated in a given bond. If for a given loading, the stress in a bond can be reduced, then the probability of its breaking will be reduced. If this occurs among a large enough number of bonds, the overall load bearing capacity of the snow can be increased.

The coordination number is also a measure of the relative mobility of ice grains within the snow. The ability of a grain to move diminishes as its coordination number increases. The coordination number depends upon the relative spacing of the ice grains. An increase in coordination number may indicate a decrease in intergranular spacing—another factor affecting grain mobility—which is reflected in the overall deformation observed.

From these considerations, it appears that to use microstructure as a basis for understanding snow behaviour, it is necessary to have a means to observe, measure and quantify the related parameters. Mathematical morphology and quantitative stereology provide the means.

3. DEFINITIONS FOR BONDS AND NECKS

In this section, definitions describing snow, its microstructural parameters and the corresponding stereological relations are given. The description used to characterise snow is due to Hansen and Brown[2]. In developing their multiaxial constitutive model, snow was considered to be a three phase material. The phases consisted of an air phase, ice grain phase and neck phase. The air phase is the material pore space, the ice grain phase consists of the individual ice grains excluding the intergranular bonding regions. The neck phase is made up of all the solid phase comprising the intergranular bonding regions. The intergranular bonding region was taken to be the constricted region joining two ice grains and lying between the points at which the curvature changes from convex to concave with respect to the outward surface normal.

A generally accepted criterion for the existence of a bond was given by Kry[5]. He specified that, for a bond to exist, a minimum constriction of 30 per cent must exist between connected segments of ice in a surface section plane, the constriction must be present on two opposing sides, and these constrictions must point approximately towards one another. This definition is too restrictive to characterise the variety of bond geometries that commonly occur. Grains may bond and yet exhibit only one convex surface which precludes opposing constrictions. It is also possible to envision bonded grains which have two opposing convex surfaces but yet the normals do not point towards one another. To account for the many configurations of bonds which occur, a more general definition of a bond is needed.

The location of a bond is determined by locating the disk of minimum diameter with center on the skeleton lying between two connected grains, as indicated in Fig. 1. The skeleton of a connected set of grains, G, consists of a series of line segments which contain the radii of all maximal disks contained in G. This sequence of line segments form a centre line of the bonded grains. Making the analogy between the skeleton and the ridge lines of a chain of mountains, each point x of the skeleton being the value of a disk of radius $r(x)$, the skeleton will have a sequence of peaks and saddles. If the lowest saddle lying between two peaks has a diameter of radius less than 0.7 of the smaller of the two peaks, then this saddle corresponds to a bond. Once the location of a bond has been determined, the ends of the neck can be located by finding the points (x_n, y_n) adjacent to the bond, at which the skeleton curvature changes from concave to convex. The end points of the end segment are then found by locating the intersections of the maximal disk centred at (x_n, y_n) with the necked region perimeter.

The basic geometry of these features is shown in Fig. 2. If planes are passed through the neck region forming all possible cross-sections, then the bond will be that cross-section which has minimum area. The plane cutting the bond is shown in Fig. 2, where the perimeter of the hatched area is the trace of the surface on the plane and the hatch is the bond. This separates the neck region into a left and a right half.

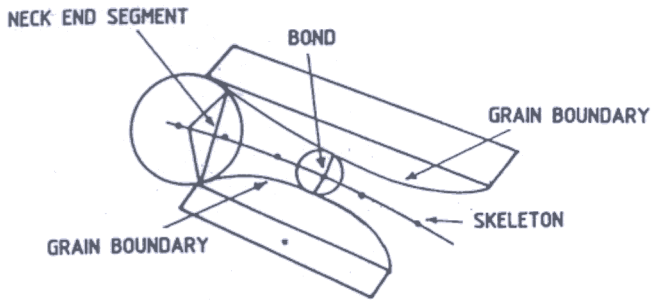

Figure 1 Skeleton and maximal disks corresponding to the bond and end segment of the left half neck.

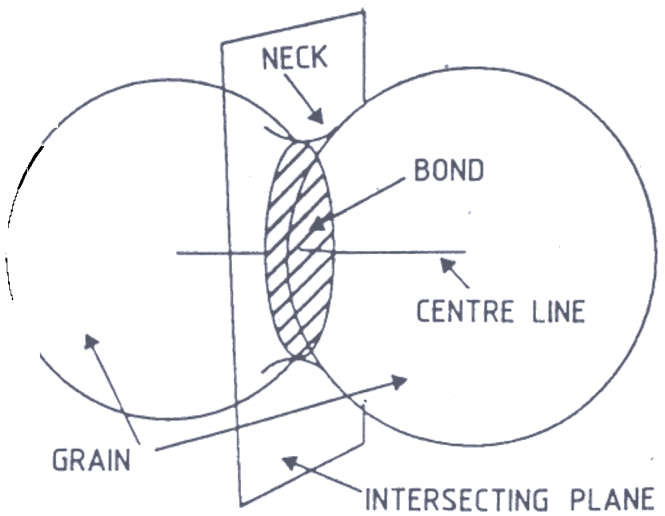

Figure 2. Three-dimensional view of two bonded grains. The bond between the grains is the hatched area and is shown projected onto an intersecting plane.

If the plane containing the bond is translated to the left along the centre line joining the grain centres, at a distance h_l from the bond, the plane will pass through locus of points on the grain surface where the curvature parallel to the centre line changes from concave to convex. This region between the bond and the plane at h_l is the left half of the neck. If the plane is translated to the right of the bond, a similar procedure will give a distance h_r defining the right end of the neck. The result of this procedure as would be seen on a cross-section taken throughout the center line is shown in Fig. 3. The total length of the neck, h, is given by $h = h_l + h_r$. It was suggested by Kry[5] that the bond can be modelled as a disk. This seems reasonable. In the cross-section plane there would be a tendency to minimise the perimeter length for a given cross-section area. The figure which satisfies this minimisation is a circular disk.

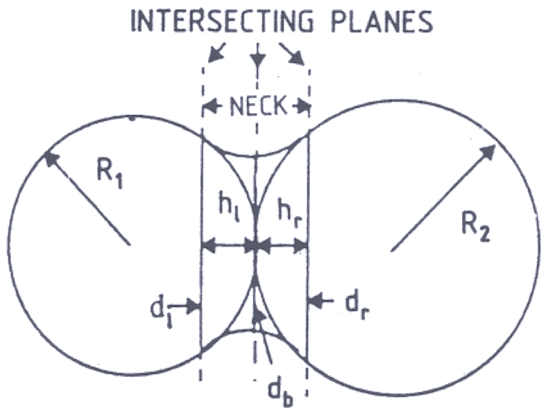

Figure 3. Cross-section through a bonded grain pair. R_1 and R_2 are the grain radii. Neck is the region between the two planes intersecting the grains at a distance h_l and h_r from the bond. d_l and d_r are the diameters of the neck ends and d_b is that of the bond.

The neck is modelled by considering it to be composed of a left and a right half. The actual model is that of a single half. From the geometry of Figs 2 and 3, along with the description of the ends, half the neck is then the volume bounded by the area of the grain intersected by the plane at h_l approximated by a circular disk of diameter d_l, say, and the bond of diameter d_b. The perimeter of the disk at h_l corresponds to the locus of points where the surface curvature changes from concave to convex. One of the main reasons for studying the neck itself is to determine its growth during plastic deformation. This requires a description which will allow for measurement of neck lengths. A first order approximation of half the neck is obtained by taking it to be a truncated cone of height h_l.

From quantitative stereology, expressions can be obtained relating measurements made on two-dimensional cross-sections of a snow sample, in particular bonded grain pairs, to the average three-dimensional values of the neck half heights, end diameter and bond diameter. The intersection of the sectioning plane with the neck ends and bond produce a linear trace on the surface section. We can measure the corresponding line segments by locating the end points on the perimeter of the bonded grain pair (Fig. 4). The stereological relation for the mean three-dimensional diameter of a disk, randomly oriented and uniformly distributed, in terms of the two-dimensional diameters given by Fullman[6] is :

$$R = \frac{\pi}{4E_2} \qquad (1$$

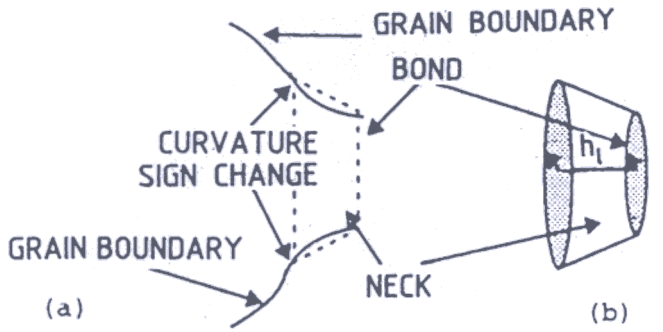

Figure 4. Two and three-dimensional neck configurations. The dotted lines forming a trapezoid are the cross-section of a neck as seen on a surface section. It is generated by determining the corresponding corner points lying on the surface boundary.

The subscripts indicate the dimension of the variable. E_2 is called the harmonic mean and is given by

$$E_2 = \frac{1}{N} \sum_i \frac{1}{d_i} \tag{2}$$

where N is the number of measurements and d_i is the ith two-dimensional diameter.

The mean height of a truncated cone can be obtained as follows. Denote the ratio of total surface area of a cone to the containing volume by S_v. This ratio can be measured by counting the number of intercepts of a test line with the perimeter of the cone cross-section seen in the surface section. The required relation which is valid for any particle[7] is given by

$$S_v = 2N_L \tag{3}$$

where N_L is the number of boundary intercepts per total length of test line. Multiplying this by the inverse of the cone volume fraction, $(V_v)^{-1}$, the left hand side of the equation becomes

$$S_v V_v^{-1} = \frac{\bar{S}}{\bar{V}} \tag{4}$$

in which $\bar{S}$ is the mean surface area of the truncated cones and $\bar{V}$ is their mean volume. The right hand side of Eqn (4) becomes

$$2N_L V_v^{-1} = 2N_L (\bar{A}_A)^{-1} \tag{5}$$

where $\bar{A}_A$ is the mean area fraction of the cross-section of truncated cones. Equality between A_A and V_v is shown in Weibel book[7]

Combining Eqns (4) and (5)

$$\frac{\bar{S}}{\bar{V}} = 2N_L (\bar{A}_A)^{-1} \tag{6}$$

The surface area of a truncated cone is given by

$$S = \pi \{r_1^2 + r_2^2 + (r_1 + r_2) \sqrt{(r_1 - r_2)^2 + h^2}\} \tag{7}$$

and volume by

$$V = \frac{\pi}{3}(r_1^2 + r_2^2 + r_1 r_2)h \tag{8}$$

where r_1 and r_2 are respectively the radii of the base and truncated end of the cone and h is the height. If these variables are replaced by their mean values, equations for the mean surface area and mean volume are obtained. Substituting the resulting expressions for the mean surface area and mean volume into Eqn (6) yields

$$\frac{(\bar{r}_1^2 + \bar{r}_2^2) + (\bar{r}_1 + \bar{r}_2) \sqrt{(\bar{r}_1 - \bar{r}_2)^2 + \bar{h}^2)}}{\{ \frac{1}{3}(\bar{r}_1^2 + \bar{r}_2^2 + \bar{r}_1 \bar{r}_2)\bar{h} \}} = 2N_L (\bar{A}_A)^{-1}$$

After a bit of algebraical manipulation, this can be solved for the mean truncated cone height, $\bar{h}$, which is found to be

$$\bar{h} = \frac{ab \pm c\sqrt{b^2 + (a^2 - c^2)d^2}}{(a^2 - c^2)}$$

where a, b, c and d are given by

$$a = 2N_L (\bar{A}_A)^{-1} \quad \frac{\bar{r}_1^2 + \bar{r}_2^2 + \bar{r}_1 \bar{r}_2}{3} \tag{11}$$

$$b = \bar{r}_1^2 + \bar{r}_2^2 \tag{12}$$

$$c = \bar{r}_1 + \bar{r}_2 \tag{13}$$

and

$$d = \bar{r}_1 - \bar{r}_2 \tag{14}$$

Choice of the positive or negative sign needs to be made. To begin, consider the limiting case when $r_1 = r_2$. This gives $d=0$ and the radical then reduces to b. The new expression for $\bar{h}$ is

$$\bar{h} \quad b\frac{(a \pm c)}{(a+c)(a-c)} \tag{15}$$

with the two roots upon cancellation of common factors being

$$\bar{h}_- = \frac{b}{(a-c)} = \frac{1}{N_L(\bar{A}_A)^{-1} r_1 - 1} \tag{16}$$

and

$$\bar{h}_+ = \frac{b}{(a+c)} = \frac{1}{N_L(\bar{A}_A)^{-1} r_1 + 1} \tag{17}$$

Measurements indicate that $N_L(\bar{A}_A)^{-1} r_1$ may be less than 1. Thus in one case $\bar{h}_+$ yields a physically meaningless negative height. On the other hand as $N_L(\bar{A}_A)^{-1} r_1$ approaches 1, $\bar{h}_+$ goes to infinity. From this it seems reasonable to reject the positive root. It can be seen that $\bar{h}_-$ will always be positive and finite. Finally, choosing the negative root in Eqn (10), the equation for the truncated cone height becomes

$$\bar{h} = \frac{(ab-c)\sqrt{b^2+(a^2-c^2)d^2}}{(a^2-c^2)} \tag{18}$$

With the preceding discussion, the following three-dimensional variables can be calculated: the bond diameter D_b, the diameters of the neck ends, D_l and D_r and from these and Eqn (18), the neck height, $h = h_l + h_r$. The measurements required to determine the diameters are the two-dimensional diameters d_b, d_l and d_r, obtained from the surface section of the grains and necks. The skeletonising routine, discussed later, can be used to locate and measure d_b, d_l and d_r.

4. SKELETONS

Under the assumption that bonds can be approximated by circular disks, as well as the end surfaces of the neck, the following equation relating two-dimensional radii in the plane to the three-dimensional means, is derived by Fullman[6]

$$\bar{R}_3 = \frac{\pi}{4E} \tag{19}$$

where E is the harmonic mean. It is defined by

$$E = \frac{1}{N}\sum_{i=1}^{N}\frac{1}{2R_{2i}} \tag{20}$$

and R_{2i} is the two-dimensional radius of the bond seen on the surface section.

To obtain surface section measurements, a robust method of automated measurements is desired. The method chosen and described next, for measurement of neck length, bond diameters and radii, also yields the coordination numbers, values for characterising grain size and number of grains in a connected group. This method, known as skeletonising, transforms the connected regions of interest into a connected set of one parameter space curves. To describe the process of obtaining a skeletal representation, several definitions are needed. As the image to be measured will be digitised and displayed on a square grid, the definition of a neighbourhood of a point and the distance from a point to a neighbour are needed. The neighbourhood of a point x, as seen on a square grid, and the connectivity between it and its nearest neighbours is shown in Fig. 5. The remaining definitions will describe the properties necessary to construct an image skeleton. Let G be an open set. The skeleton of G, and $Sk(G)$ is defined to be the locus of centres of maximal discs contained in G. This definition is shown pictorially in Fig. 6. The upstream of a point x is defined[8] to be the closed set of points y in G such that

$$r\,G\,(y) = r\,G\,(x) + d\,(x, y) \text{ for } x \in G \tag{21}$$

For the closed set G, a point y upstream of x can also be characterised by the criterion: y is upstream of x if the altitude of $y>x$ and the slope from x to the two nearest neighbours of y are less than the slope from x to y.

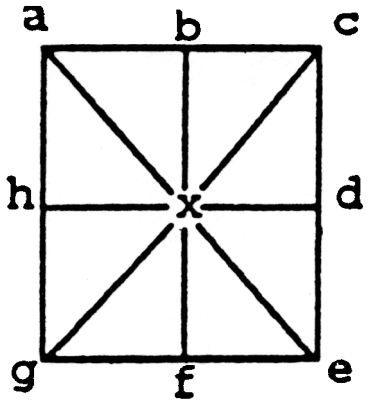

Figure 5. Euclidean distance from x to any neighbour is 1 for b, d, f, h, and $\sqrt{2}$ for a, c, e, g.

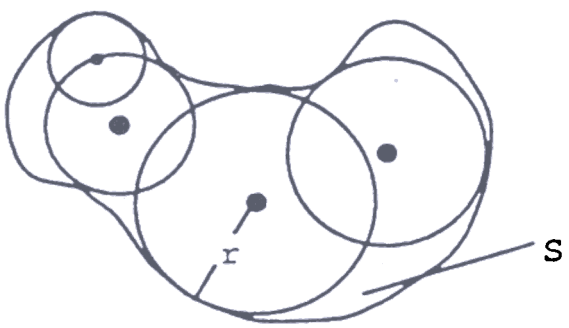

Figure 6. Examples of maximal disks contained in a set S. The dots are the disk centres.

To determine the upstream of a point x on the square grid, it is necesary to check nearest and next nearest neighbours for the positions shown in Fig. 7. The following definition is from Meyer[9]. Begin by forming a family of neighbourhoods U, coding each nearest neighbour n_i of a point x with 0 when $n_i < x$, 1 when $n_i > x$ and all possible combinations of 0's and 1's for each $n_i = x$. A point x is said to be a crest point, if: (i) all neighbours of x have code 0, and coding x with 0 would remove the only element of value 1, (ii) coding x with zero forms a bridge between elements of the neighbourhood which were not originally connected, and (iii) coding x with zero would remove the only connection between neighbours of x with value 1. An example of one neighbour configuration satisfying this definition is shown in Fig. 8.

Construction of a skeleton requires generating a distance map, detecting crest points, and finding points with upstreams. The distance map is generated by the implementation of an algorithm developed by Rosenfeld-Lay [Rosenfeld and Pfaltz[10], described in Ref. 9 1988]. An example of a distance map is shown in Fig. 9(b).

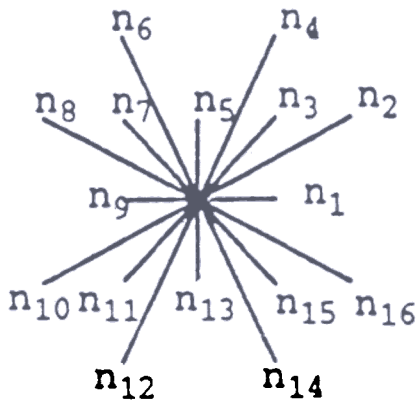

Figure 7. Sixteen neighbours of the central point.

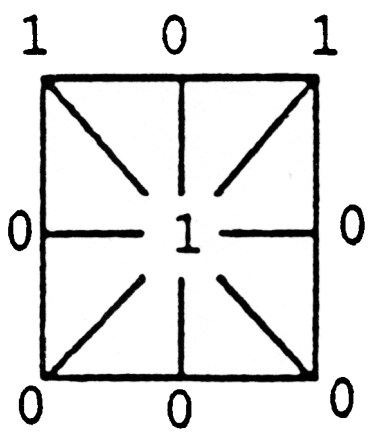

Figure 8. In this example of a configuration representing a crest point as per the definition in the text, the only connection between the two ones in the upper right and left is through the one in the centre. If this one is set to zero, then the only connection between the remaining ones is broken.

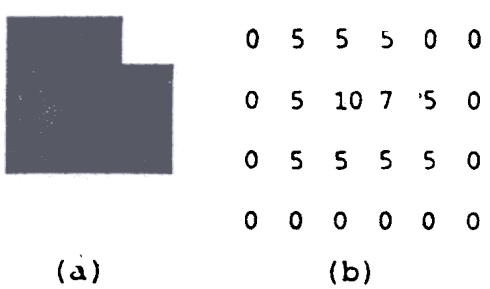

Figure 9. The distance map of Fig. 9(a), generated by Eqns (22) and (23), is shown in Fig. 9(b).

This is a two-pass algorithm. Pass one proceeds in direct video order from right to left and top to bottom. The value x is transformed into the value x^* by the following relation:

$$x^* = \min\{x, \min(a^*, b^*, c^*, d^*)\} \quad (22)$$

where a^*, b^*, c^* and d^* are previously transformed values on a square grid. The second pass proceeds from right to left and from bottom to top. The value x is transformed into x^* by the following relation:

$$x^* = \min\{x, \min(e^*, f^*, g^*, h^*)\} \quad (23)$$

where e^*, f^*, g^* and h^* are previously transformed values. The numerical of a planar figure generated by Eqns (22) and (23), can be viewed as a topographic map of the figure, where the topo-lines represent shortest distance from a figure point to the boundary.

After creating a figure of distance map, the next step is to locate and mark all crest points. By comparing the neighbourhoods of figure point with a series of templates similar to the one in Fig. 9, and marking only those which match one of the templates, the crest points of the figure can be recorded. Each template is one of the possible configurations resulting from the crest point definition. The last step required to complete the skeleton is the detection of the points with upstream which requires three passes over the current set of crest points. For each crest point, neighbours are checked to determine if one point has a slope larger than the others and if its slope is +1. Those points which satisfy the criteria are then recorded and stored with the set of crest points. The resulting skeleton of the figure in Fig. 9(a) is shown in Fig. 10.

Figure 10. The resulting skeleton of the figure in Fig. 9(a).

5. BOND DETECTION AND MEASUREMENT

Measurements concerned with locating the bonds and evaluating the diameters do not require the information contained in the dendritic structures emanating from local maxima and terminating at a local minima. Pruning removes only those points which are end points of a line segment and have only upstreams. This process is iterated in groups of three passes until no points are removed during a complete pass.

The location of a bond follows from the following description of the skeleton and grain relationship. The skeleton of a connected set of grains, G, consists of a series of line segments which contain the radii of all the maximal disks contained in G. This sequence of line segments forms a centre line or medial axis of G. Making the analogy between the skeleton and the ridge lines of a chain of mountains, each point x of the skeleton being the value of a disk of radius $r(x)$, the skeleton will have a sequence of peaks and saddles. If the saddle between two peaks has a height less than some percentage of the smaller of the two peaks then the saddle will be taken as a bond. This is implemented by traversing each point of each skeleton, recording peak and saddle values and applying the bond definition being used to successive peak and saddle values. Those that satisfy the definition are recorded for later use. Once all bonds have been found, each one is read into the equation for E [Eqn (20)], and lines representing the bonds are drawn on the image, thereby segmenting it into individual grains. The number of bonds and the mean 2-D radius are also determined at this time. By segmenting the image into individual grains, measurements concerning mean values of a single grain can be obtained. The results of skeletonising and segmenting are shown in Fig. 11.

An example of a single grain measurement is the volume weighted volume of the grains which constitute the sample. The method used is due to Gundersen and Jensen[11]. It is based upon a point-sampling algorithm. A random grid is placed on the image. The intercept length, l_0, of each grain intersected by a point of the grid is measured. The volume weighted volume is then obtained from

$$\bar{V}_v = \frac{\pi}{3} \bar{l}_o^3 \quad (24)$$

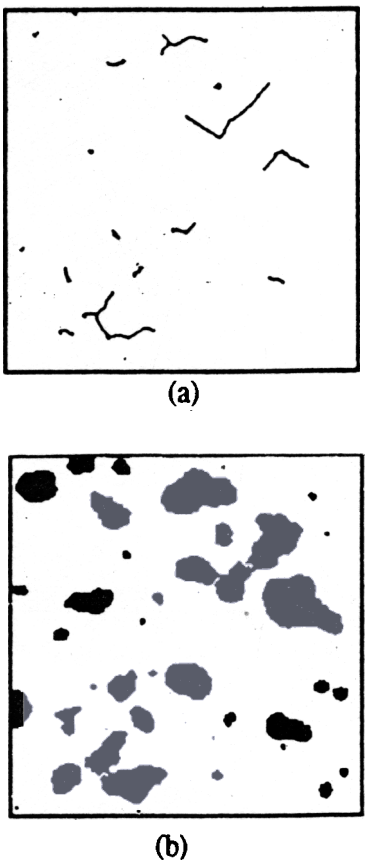

Figure 11 Figure 11(a) is the skeleton of Fig. 11(b) prior to segmenting. In Fig. 11(b) bonds are in black.

by averaging l_0 over all the measured grains. The main criteria for the validity of this method are that either each grain be convex or all points of a grain as seen on a section can be identified. Under these constraints, this technique is valid for a single surface section. The resulting value $\bar{V}_v$ is greater than or equal to the mean volume weighted by number. For grains which are nonconvex, each part of the grain intercepted by the measuring line must be measured. In this case, the value of l_0 is given by

$$l_0 = l_{0,0}^3 + 2 \sum_{i=1}^{\bar{k}} l_{0,i}^3 \qquad (25)$$

The meaning of the terms in Eqn (25) is graphically depicted in Fig. 12.

When measuring the volume weighted volume, the bonds on the segmented image unit separate the grains into individual units. From the resulting value, an estimate of the mean number of grains per volume can be obtained from

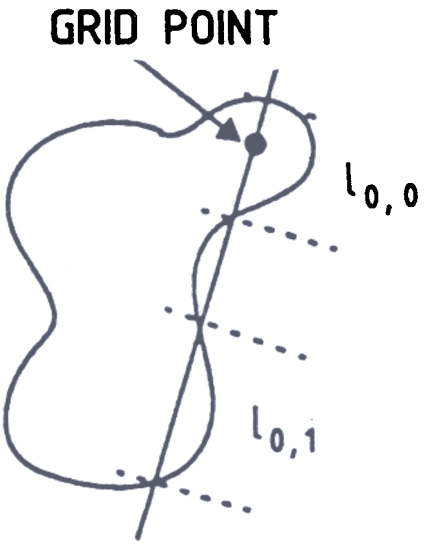

Figure 12. In this figure the measuring line intercepts the same grain several times; $l_{0,0}$ is the segment of the line passing through the grid point. Other segments of the line intersecting the grain are labelled $l_{0,i}$. In the figure $i = 1$.

$$N_v = \frac{V_v}{\bar{V}_v}$$

where V_v is the volume fraction of ice to snow. This along with the number of bonds per volume, allows the estimation of the mean 3-D coordination number. The number of bonds per unit volume can be obtained from an equation given by Fullman[6] for the number of disks per unit volume.

$$N_{bv} = \frac{8EN_{bA}}{\pi^2}$$

E is given by Eqn (20) and N_{bA} is the number of bonds per unit area. The equation for the mean 3-D coordination number is

$$\bar{N}_3 = \frac{N_{bv}}{N_v} \qquad (28)$$

Equation (28), along with the 3-D bond radius, provides two of the major parameters governing the deformation behaviour of snow. The volume measurement also provides another useful insight. This has to do with the grain mobility as a function of the number of grains in a given volume. Upon completion

of a neck length model, a measurement of the change in spacing between grains can be implemented with all the results presented.

6. APPLICATION OF THE THEORY

As an example of the application of the preceding presentation, surface section measurements taken from an ice sintering experiment are discussed. The measurements of three sections, taken from hour 0, 6 and 24 hours day are shown in Table 1. The values R_G from the table are the mean radii of the largest spheres contained in the average grain. These provide a lower bound on the actual size of the grains.

Table 1. Surface section measurement. N_L is the number of perimeter intercepts per unit length of test line, R_G is the mean radius of the maximal sphere contained in the average sized grain, and R_b is the mean three-dimensional bond radius

Hour	Density (g/mm^3)	Area fraction	$N_L(\mu)$	$R_G(\mu)$	$R_b(\mu)$
0	0.00009	0.09552	0.0038	10.46	3.92
6	0.0001	0.1141	0.00381	11.09	4.87
24	0.00021	0.22428	0.0046	17.87	8.80

Figure 11 is an example of the skeleton and segmented (bonds only) image obtained from a portion of one of the experiment's surface sections. The skeleton in Fig. 11 (a) is the pruned form of the original skeleton. The neck segmenting routine has not been completed; as a result, Fig. 11 (b) only shows the segmentation corresponding to bonds.

Table 2 shows the volume of the sphere V_G and area of the bonds A_b obtained from the values of Table 1. In the case where grains can be approximated by spheres, a procedure similar to that for obtaining the mean neck height can be used to obtain the mean sphere radius. Results of such a calculation for r_G are also shown in Table 2. The corresponding equation is

$$r_G = \frac{3}{2} A_A N_L^- \tag{29}$$

where N_L is the mean number of grain boundary intersections per unit test line length, and A_A is the area fraction of the grains. The values of volume obtained from r_G are given in the last column of Table 2.

Table 2. Parameter values calculated from values given in Table 1

Hour	$V_G(\mu)^3$	$A_b(\mu)^2$	$r_G(\mu)$	$V_{rG}(\mu)^3$
0	4792.5	48.2	18.8	28055.8
6	5718.3	74.4	22.5	47712.9
24	23923.2	243.4	36.6	205367.6

Automation of the measurement process seems to be an attainable goal as shown by the above results. These were obtained by simply indicating the particular measurement to be made, no other input was needed. The bond required only the selection of this as the task. Automation is particularly valuable for image segmentation based upon various models. Only through automation, can such a process be carried out consistently from one image to the next. The work load required to complete the task is greatly reduced. Each section required less than 5 min to complete the section measurement and hand calculations by which the volumes and area were calculated. These images were of the order of 500 by 700 pixel elements in size.

Finally, a model for the necked region for bonded particles is presented. By use of the automated methods, the end cap radii can be measured and, as a result, the neck length can be calculated. The model provides a first order approximation to the actual neck. This model could also be used to obtain the neck length even if calculations of the neck volume were based upon a model which describes the surface geometry better.

REFERENCES

1. Brown, R.L. A volumetric constitutive law for snow based on a neck growth model. *J. Appl Phys.*, 1980, **51**(1), 161-65.
2. Hansen, A.C. & Brown, R.L. The granular structure of snow: An internal-state variable approach. *J. Glaciol.*, 1986, **32**(112), 434-38.
3. Alley, R.B. Firn densification by grain-boundary sliding: A first model. *J. Phys. (Paris)*, 1987, **48**, Collq. C1, (Supplement au 3.), 249-54.
4. Edens, M.Q. & Brown, R.L. Changes in microstructure of snow under large deformations. *J. Glaciol.*, 1991, **37**(126), 193-202.

5. Kry, P.R. Quantitative stereological analysis of grain bonds in snow. *J. Glaciol.*, 1975, **14**(72), 467-77.

6 Fullman, R.L. Measurement of particle sizes in opaque bodies. 1953, *AIME*, **197**, 447-52.

Weibel, E. Stereological methods, Vol. 2. Academic Press, New York, 1980.

8. Matheron, G. Examples of topological properties of skeletons. *In* Image analysis and mathematical morphology: Theoretical advances, edited by Jean Serra. Academic Press, New York, 217-38.

9. Meyer, F. Skeletons in digital space. *In* Image analysis and mathematical morphology: Theoretical advances, edited by Jean Serra. Academic Press, New York, 1988, 257-96.

10 Rosenfeld, A. & Pfaltz, J.L. Sequential operations in digital picture processing. *J. ACM*, 1966, **13**, 471-94.

1 Gundersen, H.J.G. & Jensen, E.B. Stereological estimation of the volume-weighted mean volume of arbitrary particles observed on random sections. *Journal of Microscopy*, 1985, **128**(Pt 2), 127-42.